

Combination of microwave ablation and systemic treatments achieve a long survival time for a patient with metachronous advanced double primary lung and colon adenocarcinoma: A case report

YUN LI¹, YALI XU², SHIFENG CAI³, JINGWEN LI⁴, FANGYING RUAN⁵,
CHAORAN XIA⁵, PENG LUO⁵ and JUN LI⁶

Departments of ¹Thoracic Surgery, ²Pathology, ³Radiology and ⁴Gastroenterology,
Shandong Provincial Hospital Affiliated to Shandong First Medical University, Jinan, Shandong 250021;
⁵Zhejiang Shaoxing Topgen Biomedical Technology Co., Ltd., Shanghai 201321; ⁶Department of Oncology,
Shandong Provincial Hospital Affiliated to Shandong First Medical University, Jinan, Shandong 250021, P.R. China

Received July 27, 2023; Accepted March 7, 2024

DOI: 10.3892/ol.2024.14540

Abstract. Despite significant improvements that have been made in terms of progression-free survival and overall survival rates brought about by targeted therapy in non-small cell lung cancer (NSCLC), the emergence of drug resistance remains a limiting factor. However, a previous study has shown promising results by combining local microwave ablation (MWA) with epidermal growth factor receptor (EGFR)-tyrosine kinase inhibitor (TKI) therapy for patients with oligometastatic NSCLC. The current study presented the case of a Chinese female patient who was identified as having lung adenocarcinoma (LADC) with EGFR exon 19 deletions (Del) in January 2014, and who experienced multiple instances of oligoprogression but showed a positive response to a combination of chemotherapy, MWA and a TKI drug. First, the patient was treated with four cycles of chemotherapy (120 mg docetaxel on day 1 and 40 mg cisplatin on days 1, 2 and 3; every three weeks as one cycle) and gefitinib (Iressa; 250 mg/day), maintaining a partial response for 17 months. In August 2015, a new solitary lesion was identified in the right lung and erlotinib (Tarceva; 150 mg/day) was administered for 3 months thereafter. In response, the patient underwent ablation of both the new right lung lesion and the primary left lung lesion in January 2016. Subsequently, a treatment course consisting of six cycles of chemotherapy (0.8 g pemetrexed

on day 1 and 70 mg nedaplatin on days 1 and 2; every three weeks as one cycle) resulted in stable disease. In May 2016, the patient began treatment with osimertinib (AZD9291; 80 mg/day), resulting in a rapid shrinkage of the mediastinal lymph node after one month, which has been providing a benefit for the patient for 82 months and counting. Of note, the patient also developed metachronous colon cancer in January 2020, followed by the identification of right posterior liver metastases in February 2020 and lung metastases in May 2021 and in February 2022. To address this, the patient underwent radical resection of colon cancer and liver metastasectomy and received a combination of chemotherapy with bevacizumab, along with MWA for lung metastases. Remarkably, the patient has achieved long-term survival of 110 months. In conclusion, this case highlights the promising potential of combining MWA with systemic therapy for a patient with advanced LADC harboring EGFR exon 19 Del and metachronous lung and liver-metastasized colon adenocarcinoma. MWA effectively controlled both *in situ* oligoprogression and new oligoprogression, thereby enhancing the efficacy of systematic chemotherapy/TKI therapy. Furthermore, this case report emphasizes the importance of repeated histologic biopsies and genetic testing as reliable indicators for adjusting treatment regimens. Physicians should also remain vigilant regarding the occurrence of secondary primary carcinomas, and timely and accurate adjustments to treatment plans will be of significant benefit to patients in terms of treatment efficacy and overall quality of life.

Correspondence to: Dr Jun Li, Department of Oncology, Shandong Provincial Hospital Affiliated to Shandong First Medical University, 324 Jingwuweiqi Road, Jinan, Shandong 250021, P.R. China
E-mail: lijun201911@163.com

Key words: metachronous advanced lung and colon adeno-carcinoma, EGFR 19 exon deletion, EGFR-TKI, microwave ablation, chemotherapy

Introduction

Lung cancer continues to represent the foremost cause of cancer-associated mortality globally, with an annual death toll surpassing 1.6 million (1). Among cases of primary lung cancer, non-small cell lung carcinoma (NSCLC) accounts for 85%, with lung adenocarcinoma (LADC) being the predominant subtype, constituting 40% of cases. Patients

with stage IV NSCLC, however, have a dismal prognosis, with a five-year survival rate ranging from a mere 1-10% (2). Although traditional chemotherapy, targeted therapy, immunotherapy and local treatments have all been employed to combat metastatic NSCLC, the emergence of drug resistance curtails the overall efficacy of chemotherapy, targeted therapy and immunotherapy interventions (3).

In the Chinese population, mutations of the epidermal growth factor receptor (EGFR) have been recognized as the most prevalent driver of oncogenic mutations in patients with NSCLC, exhibiting a prevalence rate of 47.5%. These mutations are primarily manifested in exons 18, 19, 20 and 21, with deletions in exon 19 (19Del) and the exon 21 L858R mutation accounting for 85-90% of the cases (4). Of note, patients with NSCLC harboring the EGFR 19Del and L858R mutations showcase favorable responses to EGFR-tyrosine kinase inhibitors (TKIs) (5). In line with the 2022 National Comprehensive Cancer Network guidelines, osimertinib, erlotinib and gefitinib are recommended as category 1 treatment options for patients with confirmed EGFR 19Del or the L858R mutation (6). A common phenomenon in patients with NSCLC with EGFR mutations is oligoprogression, occurring in 30-50% of cases during targeted therapy, and at an even higher rate in patients receiving a combination of chemotherapy and immunotherapy (7). It is considered that local treatment options targeting these oligoprogressive lesions are able to eradicate insensitive and drug-resistant clones, potentially restoring treatment sensitivity (8). Local thermal ablation, a precise and minimally invasive technique, may be applied in patients with both early-stage and metastatic NSCLC with tumors ≤ 3 cm. The advantages of local thermal ablation over open surgery include shorter hospital stays, reduced risks, minimized blood loss, manageable or moderate pain levels, limited impact on lung function and the possibility of repeated treatments (9). Combining microwave ablation (MWA) with TKI treatment has led to significant improvements in both progression-free survival (PFS) and overall survival (OS) rates for patients with oligometastatic NSCLC. Of note, in a study by Wei *et al* (10), compared with the single-agent group, the MWA consolidation group exhibited a markedly enhanced PFS time (34.8 vs. 16.7 months, respectively) and OS time (22.7 vs. 12.9 months, respectively). The present case report describes a patient with LADC featuring EGFR 19Del mutations who experienced multiple instances of oligoprogression, but displayed a favorable response to a combination therapy comprising MWA, chemotherapy and TKI drugs. In addition, the patient had a history of metachronous colon cancer, along with liver and lung metastases spanning over 2 years. The treatment regimen included radical resection of bowel cancer, liver metastasectomy, chemotherapy for bowel cancer combined with bevacizumab and ablation for lung metastases. Remarkably, the patient has achieved a long-term survival duration of 110 months and remained alive without evaluable lesions on CT imaging.

Case report

In January 2014, a 50-year-old Chinese female non-smoker with no family history of cancer presented at Shandong Provincial Hospital Affiliated to Shandong First Medical

University (Jinan, China) with a persistent cough lasting over 10 days. During the physical examination, an enlarged, firm lymph node measuring 1 cm in diameter was detected in the left supraclavicular region, which was confirmed by computed tomography (CT) (Fig. 1A). In addition, CT scan of the chest revealed a 2.5x1.7 cm pulmonary nodule in the left hilum of the superior lobe (Fig. 1B and C). Of note, diffuse Millet grain-like nodules were observed in both lungs, indicating potential metastasis (Fig. 1D).

Following the biopsy on the lymph node in the left supraclavicular region, the patient was diagnosed with LADC (Fig. 1E), specifically classified as clinical stage cT1N3M1 (cIVB, IASLC 7th edition of the TNM Classification for Lung Cancer) (11). The subsequent reverse transcription-quantitative (RT-q)PCR gene testing revealed the presence of EGFR 19Del. A treatment plan was initiated, starting with four cycles of chemotherapy (120 mg docetaxel on day 1 and 40 mg cisplatin on days 1, 2 and 3; every three weeks as one cycle). This regimen led to a partial response (Fig. 2A, Table I), as assessed according to the Response Evaluation Criteria in Solid Tumors version 1.1 (RECIST 1.1) criteria and the patient was subsequently treated with gefitinib (Iressa; 250 mg/day), the patient further improved on gefitinib, maintaining progression-free survival (PFS) compared to the end of chemotherapy treatment for 16 months (Fig. 2B, Table I).

However, in August 2015, the primary nodule in the left lung was found enlarged (Fig. 2C, Table I), and a new solitary lesion was identified in the right lung, indicating disease progression (Fig. 2D, Table I). Despite the progression, biopsy and RT-qPCR gene testing of this new lesion still confirmed the presence of LADC with EGFR exon 19Del only. Before 2016, next-generation sequencing (NGS) was not available in hardly any hospitals in China, and thus, only PCR was used for tumor gene testing. The sample collected in August 2015 was confirmed by NGS testing in September 2019, indicating that the patient harbored both EGFR exon 19Del and EGFR exon 20 T790M mutation, which provided an explanation of why the patient showed progression at this time (Table II). In response, the patient underwent ablation of both the new right lung lesion (Fig. 2E) and the primary left lung lesion in January 2016 (Fig. 2F). Subsequently, a treatment course consisting of six cycles of chemotherapy (0.8 g pemetrexed on day 1 and 70 mg Nedaplatin on days 1 and 2; every three weeks as one cycle) resulted in stable disease (Fig. 3A). Erlotinib (Tarceva; 150 mg/day) was administered for 3 months thereafter (Fig. 3B, Table I). However, a CT scan in April 2016 revealed another new nodule in the right lung and enlargement of one mediastinal lymph node (Fig. 3C). The subsequent pathology report of the puncture biopsy of the lesion confirmed LADC with EGFR 19Del by PCR at that time and EGFR 19Del as well as EGFR exon 20 T790M mutations through NGS testing in 2019 (Table II). The new right lung lesion was ablated just after biopsy in May 2016 (Table I, Fig. 3D).

Subsequently, in May 2016, the patient began treatment with osimertinib (AZD9291; 80 mg/day), resulting in rapid shrinkage of the mediastinal lymph node after one month. The treatment proved effective, continuing to provide a benefit for the patient for 82 months (Fig. 4). Of note, no evaluable lesions were detected since the patient started treatment with osimertinib. In September 2017, a blood RT-qPCR test for EGFR exon

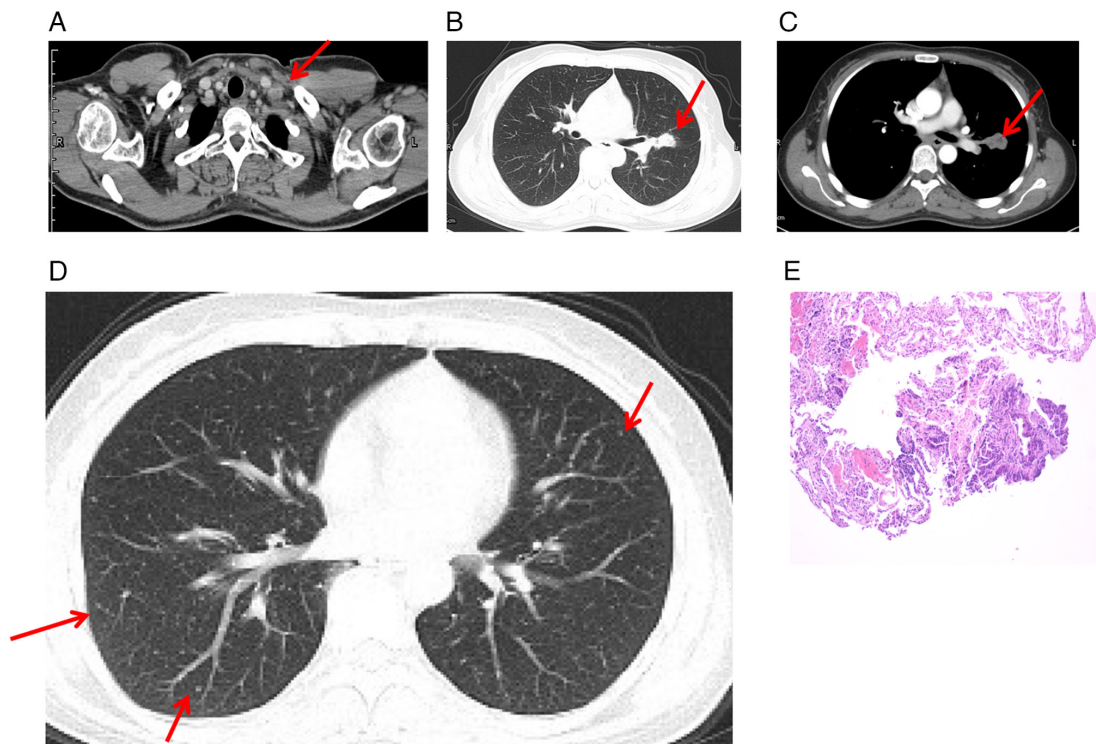


Figure 1. Diagnosis of the patient with NSCLC in January 2014. (A) CT scan revealed an enlarged left supraclavicular lymph node (arrow). (B and C) CT scan of the chest showed a pulmonary nodule measuring 2.5x1.7 cm in the left hilum of the superior lobe; the arrows point at the nodule in (B) the lung window and (C) abdomen window. (D) Diffused millet grain-like nodules in both lungs on CT suggesting lung metastasis (arrows). (E) Hematoxylin and eosin staining (magnification, x200) confirmed that the patient had NSCLC adenocarcinoma. CT, computed tomography; NSCLC, non-small cell lung cancer.

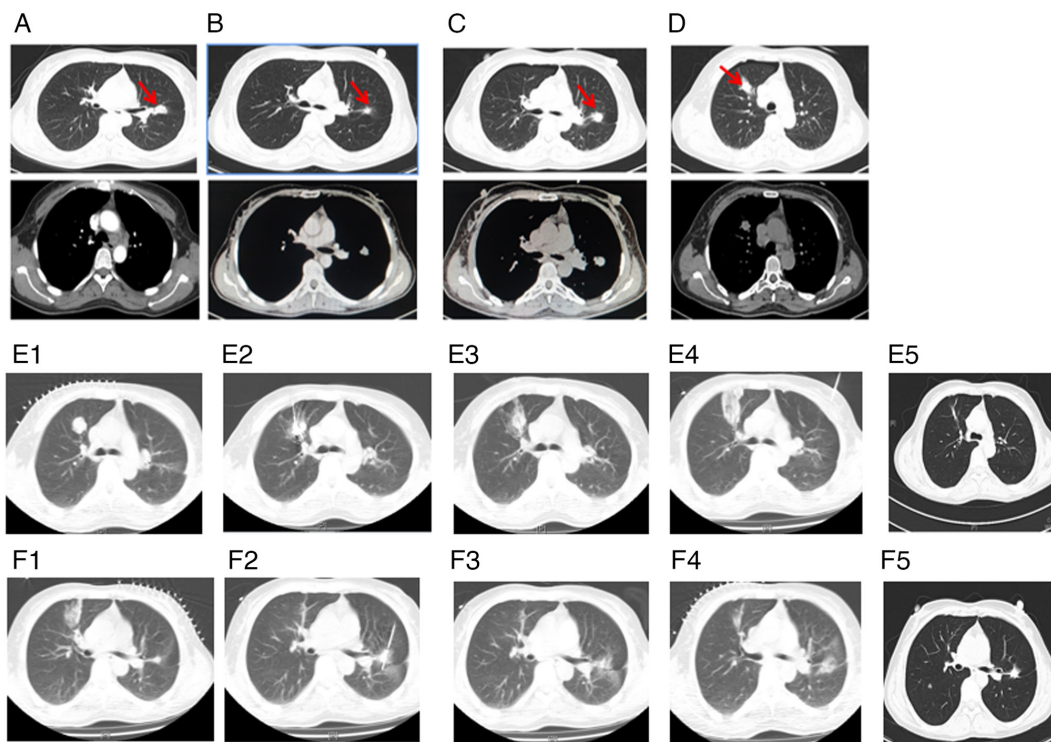


Figure 2. Lung CT scans indicating the tumors of the patient during gefitinib treatment, as well as ablations after progression. (A) March 2014: Before gefitinib treatment and at the end of the first-line chemotherapy treatment (arrow points at the primary nodule in the left lung). (B) September 2014: 6 months after gefitinib treatment (arrow points at the shrunk primary nodule in the left lung). (C) August 2015: 17 months after gefitinib treatment (arrow points at the enlarged primary nodule in the left lung). (D) August 2015: 17 months after gefitinib treatment (arrow points at the new nodule in the right lung). (E) Data pertaining to microwave ablation treatment of the right lung lesion in January 2016. (E1) Intraoperative positioning of right lung ablation. (E2) Right lung ablation procedure. (E3) Immediate scan after right lung ablation. (E4) One week after right lung ablation. (E5) >5 years after ablation. (F) Data pertaining to microwave ablation treatment on left lung lesion in January 2016. (F1) Intraoperative positioning of left lung ablation. (F2) Left lung ablation procedure. (F3) Immediately after left lung ablation. (F4) Three months after left lung ablation. (F5) >5 years after ablation. CT, computed tomography.

Table I. Timeline of the clinical course.

Time-point	Tumor location	Testing and results	Treatment
January 2014	Left superior lobe	RT-qPCR analysis: EGFR exon 19Del.	Four cycles chemotherapy (120 mg docetaxel on day 1, 40 mg cisplatin on days 1,2,3; every three weeks as one cycle), then gefitinib (Iressa; 250 mg/day) and ablation.
August 2015	A new solitary lesion right lung	RT-qPCR in August 2015: Adenocarcinoma with EGFR exon 19Del; examination by NGS in September 2019: EGFR 19Del and EGFR exon 20 T790M.	Six cycles of chemotherapy (0.8 pemetrexed on day 1 and 70 mg Nedaplatin on days 1 and 2; every three weeks as one cycle), then erlotinib (Tarceva; 150 mg/day) and ablation.
April 2016	Another new nodule in the right lung	RT-qPCR in January 2016: Adenocarcinoma with EGFR exon 19Del; examination by NGS in September 2019: EGFR 19Del and EGFR exon 20 T790M.	Ablation in May 2016; osimertinib (AZD9291; 80 mg/day).
January 2020	Colonoscopy identified multiple polyps in the cyclointestinal neoplasm located 22-26 cm from the anus	Colonoscopy; pathology confirmed primary colon adenocarcinoma. IHC results showed positive expression of <i>MLH1</i> , <i>MSH2</i> , <i>MSH6</i> and <i>PMS2</i> , whereas <i>PDL1</i> expression was negative. The NGS test conducted on this specimen revealed distinct mutations in <i>KRAS</i> , <i>PIK3CA</i> , <i>PTEN</i> , <i>APC</i> , <i>TP53</i> , <i>TSC1</i> and <i>AMER1</i> .	In January 2020, a laparoscopic sigmoidectomy was performed. Following the surgery, the patient underwent oxaliplatin (200 mg on day 1) and capecitabine (2.0 g, bid, on days 1-14) chemotherapy, every three weeks as one cycle, while continuing treatment with osimertinib.
February 2020	A 1.07x0.95 cm mass in the right posterior liver	MRI scanning	Five cycles of chemotherapy (200 mg oxaliplatin on day 1 and 2.0 g capecitabine, bid, on days 1-14) and four cycles of bevacizumab (7.5 mg/kg;) every three weeks as one cycle before undergoing hepatic metastasectomy in June 2020.
May 2021	Several newly enlarged small pulmonary nodules in the bilateral lungs; pelvic MRI identified a new abnormal focus in the right posterior lobe of the liver	In May 2021, a percutaneous thoracic needle biopsy guided by MRI was performed to obtain tissue specimens from the lung nodule. The biopsy revealed a small amount of adenocarcinoma tissue. IHC analysis showed weak CDX2 expression, negative CK7 expression, positive CK20 expression, negative napsinA expression, partial SATB2 expression and negative TTF1 expression.	Oxaliplatin (200 mg on day 1), raltitrexed (5 mg on day 1) and bevacizumab (7.5 mg/kg; every three weeks as one cycle) for six cycles. Subsequently, the treatment regimen was adjusted to include raltitrexed, bevacizumab and osimertinib. Notably, the liver metastasis disappeared based on the MRI examination conducted in November 2022.

Table I. Continued.

Time-point	Tumor location	Testing and results	Treatment
February 2022	A small pulmonary nodule showed slight enlargement, prompting an ablation procedure and a subsequent biopsy	The pathology report confirmed adenocarcinoma, although the primary site of origin could not be determined.	Ablation and treatment with AZD9291, bevacizumab and capecitabine up to the present time.

NGS, next-generation sequencing; EGFR, epidermal growth factor receptor; bid, twice daily; Del, deletion; RT-qPCR, reverse transcription-quantitative PCR; IHC, immunohistochemistry; MLH1, MutL homolog 1; MSH2, MutS homolog 2; PMS2, PMS1 homolog 2; KRAS, Kirsten rat sarcoma viral oncogene family; PIK3CA, phosphatidylinositol 3-kinase p110 alpha; PTEN, phosphatase and tensin homolog; APC, adenomatous polyposis coli; TP53, tumor protein 53; TSC1, tuberous sclerosis complex 1; AMER1, APC membrane recruitment 1.

Table II. NGS genetic testing results.

Time-point samples were obtained	Tumor position	Gene mutation item	Mutation status
August 2015 (the sample was confirmed by NGS testing in September 2019)	Right lung	EGFR EGFR TP53 Tumor mutational burden Microsatellite stable status	Exon 19Del (E746-A750Del) Exon 20 T790M Exon 8 R282W 5.6 muts/Mb Microsatellite stable
April 2016 (the sample was confirmed by NGS testing in September 2019)	Left lung	EGFR EGFR Tumor mutational burden Microsatellite stable status	Exon 19Del (E746-A750Del) Exon 20 T790M 7.5 muts/Mb Microsatellite stable
January 2020	Rectal colon	KRAS PIK3CA PTEN APC APC TP53 TSC1 AMER1 Tumor mutational burden Microsatellite stable status	G13D1 (exon 2) M1043I (exon 21) C.635-1G>A (splice site changes) K560* (exon 14) K1551* (exon 16) R248W (exon 7) R1097H (exon 23) R353* (exon2) 5.1 muts/Mb Microsatellite stable

NGS, next-generation sequencing; EGFR, epidermal growth factor receptor; Del, deletion; muts, mutations; Mb, million base pair; KRAS, Kirsten rat sarcoma viral oncogene family; PIK3CA, phosphatidylinositol 3-kinase p110 alpha; PTEN, phosphatase and tensin homolog; APC, adenomatous polyposis coli; TP53, tumor protein 53; TSC1, tuberous sclerosis complex 1; AMER1, APC membrane recruitment 1.

19Del and EGFR exon 20 T790M yielded negative results. Lung tumor markers are substances that can be measured in the body to help diagnose and monitor the progression of lung cancer. In the regular dynamic follow-up for a series of lung tumor markers [carcinoembryonic antigen (CEA), cancer antigen 125, squamous cell carcinoma antigen, neuron-specific enolase, cytokeratin 19 fragment and pro-gastrin-releasing peptide have been tested numerous times from January 2014 during treatment. However, in January 2020, the level of the

CEA was found to be significantly increased to 22.2 ng/ml, surpassing the normal range of <5.0 ng/ml (Fig. 5A and B). This increase prompted a CT scan, which revealed significant inhomogeneous wall thickening of the sigmoid colon, with the thickest wall measuring-1.8 cm (Fig. 6A).

The colonoscopy results did not reveal abnormal signs in the ileocecus area (Fig. 6B). Colonoscopy confirmed the presence of a cyclointestinal neoplasm located 22-26 cm from the anus. Views with different angles of this neoplasm are

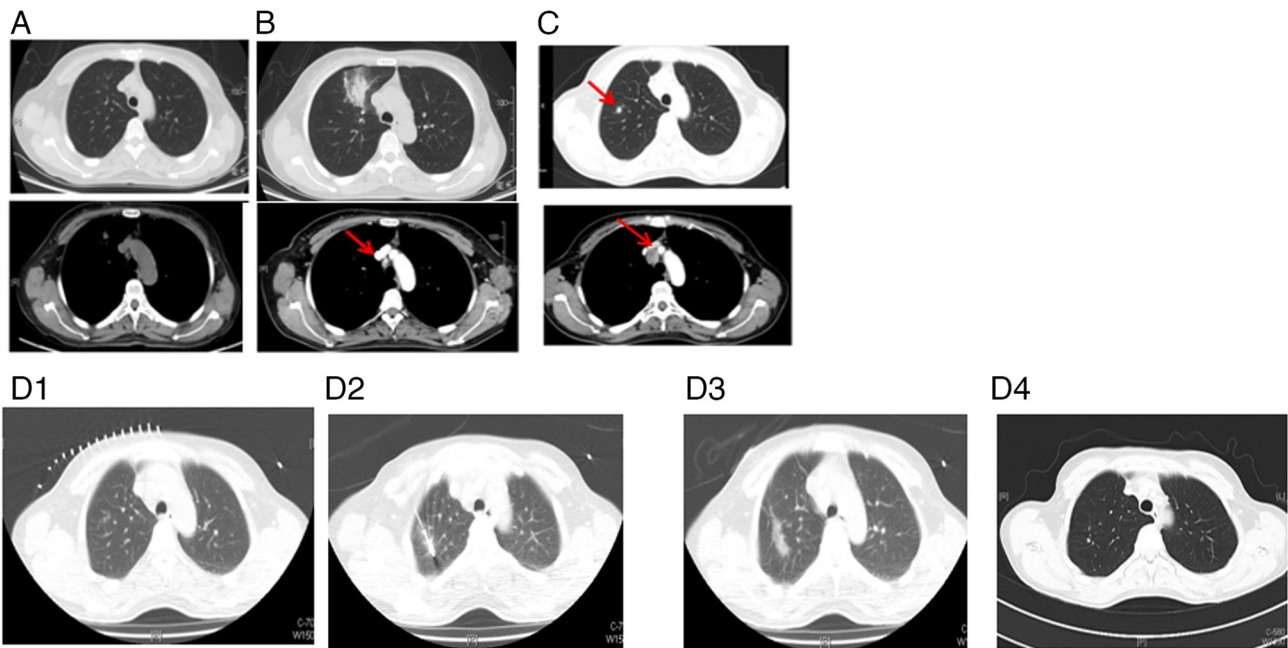


Figure 3. Lung CT scans, indicating the tumors of the patient before and after erlotinib treatment, as well as ablation after progression. (A) January 2016: Before erlotinib treatment and at the end of the second-line chemotherapy treatment. (B) February 2016: One month after erlotinib treatment (arrow points at the mediastinal lymph node). (C) April 2016: Three months after erlotinib treatment (arrow points at the new nodule in the right lung and enlarged mediastinal lymph node). (D) Data pertaining to microwave ablation treatment of the right lung lesion in May 2016. (D1) Intraoperative positioning of right lung ablation. (D2) Right lung ablation procedure. (D3) Immediate scan after right lung ablation. (D4) One week after right lung ablation. CT, computed tomography.

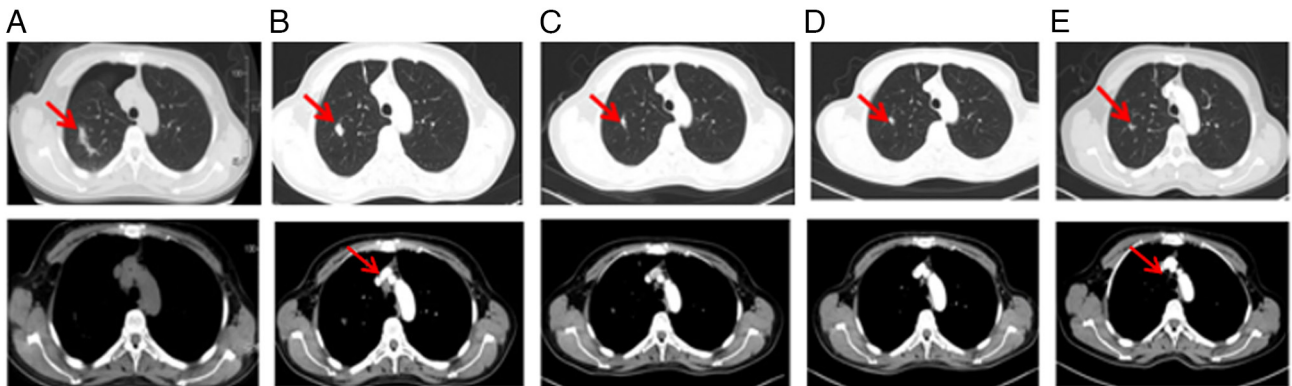


Figure 4. Lung CT scans indicating the tumors of the patient before and after osimertinib treatment. (A) May 2016: Before osimertinib treatment and at the end of second-line chemotherapy treatment (arrow points at the ablated right lung lesion and enlarged mediastinal lymph node). (B) June 2016: One month after osimertinib treatment (arrow points at the ablated right lung lesion and shrunk mediastinal lymph node). (C) November 2016: Six months after osimertinib treatment (arrow points at the ablated right lung lesion). (D) November 2018: 30 months after osimertinib treatment (arrow points at the ablated right lung lesion). (E) March 2023: 82 months after osimertinib treatment (arrow points at the ablated right lung lesion and shrunk mediastinal lymph node).

shown in (Fig. 6C1-C4), with the pathology results confirming primary colon adenocarcinoma. Additionally, multiple polyps were identified within the colon and rectum (Fig. 6D). In January 2020, a laparoscopic sigmoidectomy was performed under general anesthesia. Pathological examination revealed moderately differentiated adenocarcinoma, with a mass size of 4x0.8 cm, indicating primary colon adenocarcinoma (Fig. 6E). Malignant cells had invaded the serosa and metastasized to peri-intestinal lymph nodes (1/10), along with the formation of a tumor nodule measuring 0.3 cm in diameter in the lymph node. Immunohistochemistry (IHC) results showed positive expression of the DNA mismatch repair protein mutL homolog 1 (MLH1), MutS homolog 2 (MSH2), MutS homolog

6 (MSH6) and PMS1 homolog 2 (PMS2), whereas the expression of programmed death-ligand 1 (PD-L1) was negative (Fig. 7). The NGS test conducted on this tumor specimen revealed distinct mutations in the genes KRAS, phosphatidylinositol-4,5-bisphosphate 3-kinase catalytic subunit alpha, phosphatase and tensin homolog, adenomatous polyposis coli (APC), tumor protein p53, tuberous sclerosis 1 and APC membrane recruitment protein 1, differing from those found in the patient's lung cancer specimens (Table II). These findings suggested the presence of metachronous lung and colon adenocarcinoma, with the tumor exhibiting microsatellite stability and a low tumor mutational burden. Following the surgery, the patient underwent oxaliplatin (200 mg on day

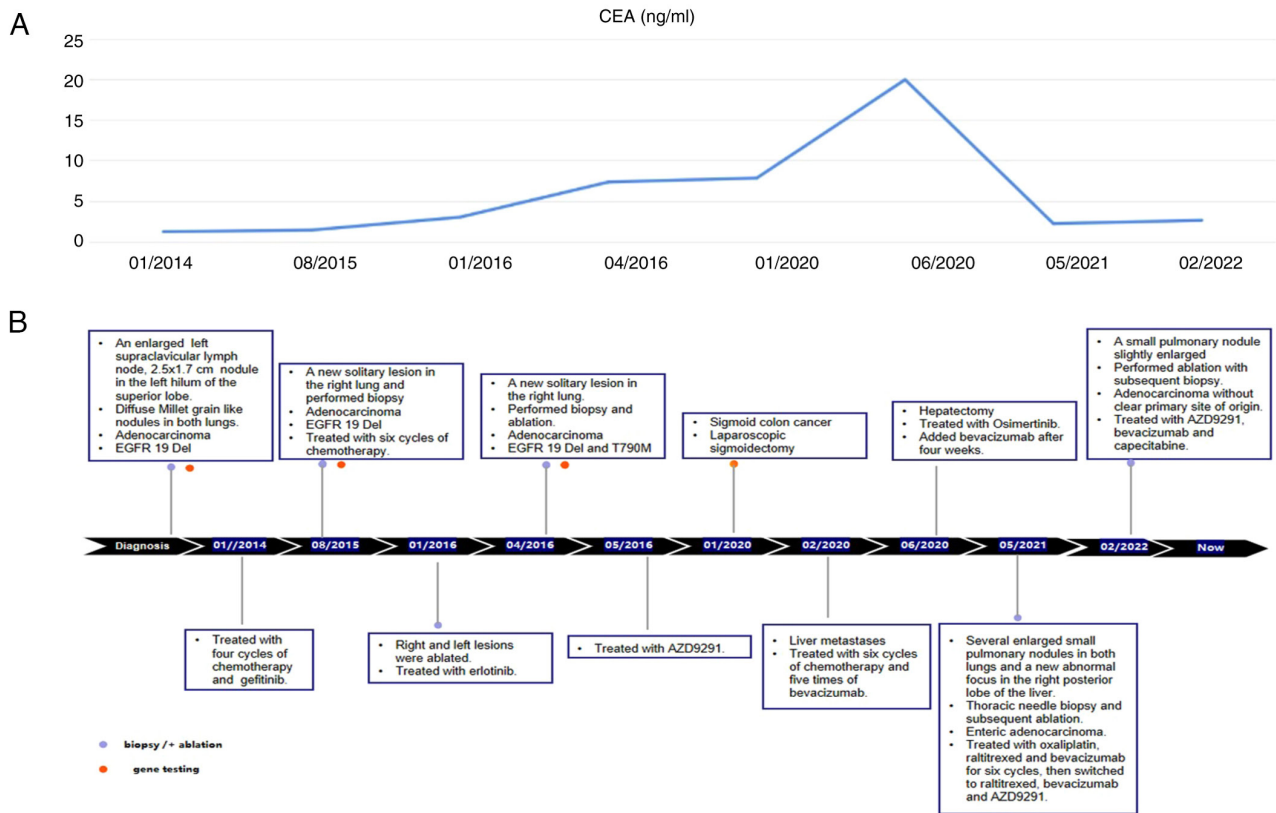


Figure 5. Treatment course of the patient and CEA levels. (A) Line chart showing changes in the levels of the serum tumor biomarker CEA during the course of treatment. (B) Timeline of the clinical course.

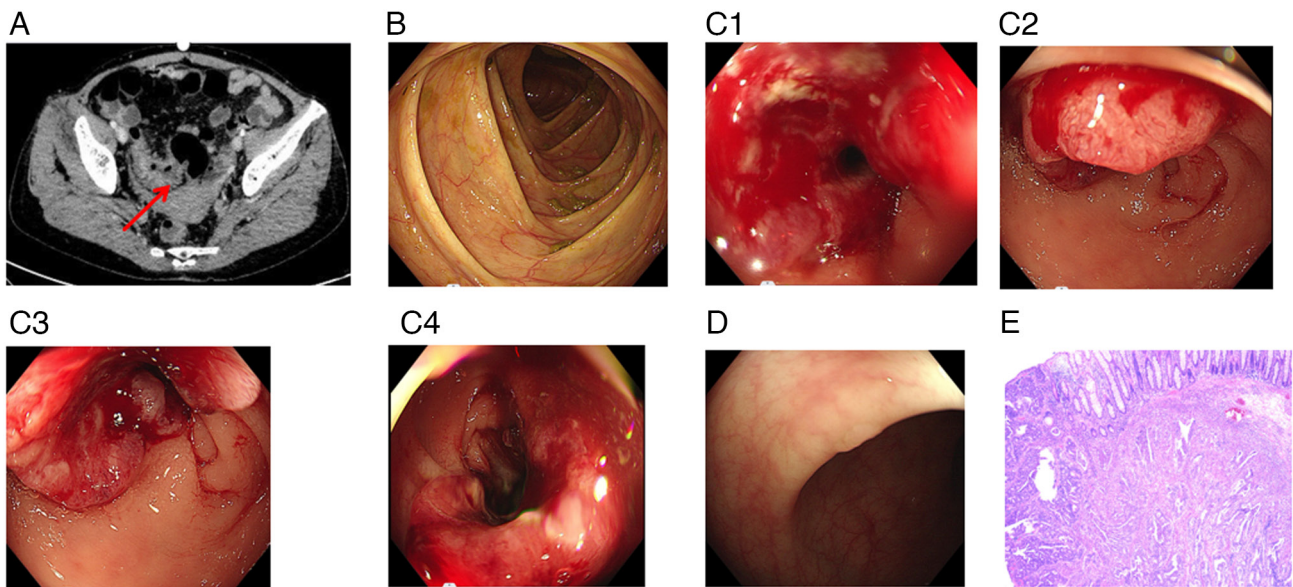


Figure 6. Clinical checks identified sigmoid colon cancer. (A) The CT scan revealed significant inhomogeneous wall thickening of the sigmoid colon wall, and the thickest wall size was measured to be ~1.8 cm. (B) No abnormal signs were identified in the ileocecus area. (C) One cyclointestinal neoplasm was identified located 22-26 cm from the anus (the size of this neoplasm was not provided in the colonoscopy report). C1, C2, C3 and C4 are the different angles of this neoplasm when biopsy was performed. (D) Arrow points at one of several polyps found in the colon and rectum. (E) The pathology result of the colonoscopy biopsy specimen was colon adenocarcinoma.

1) and capecitabine [2.0 g twice daily (bid), days 1-14, every three weeks as one cycle] chemotherapy, while continuing treatment with osimertinib.

In February 2020, 43 days after the sigmoidectomy, a follow-up magnetic resonance image (MRI) of the pelvic cavity, which had never been performed before

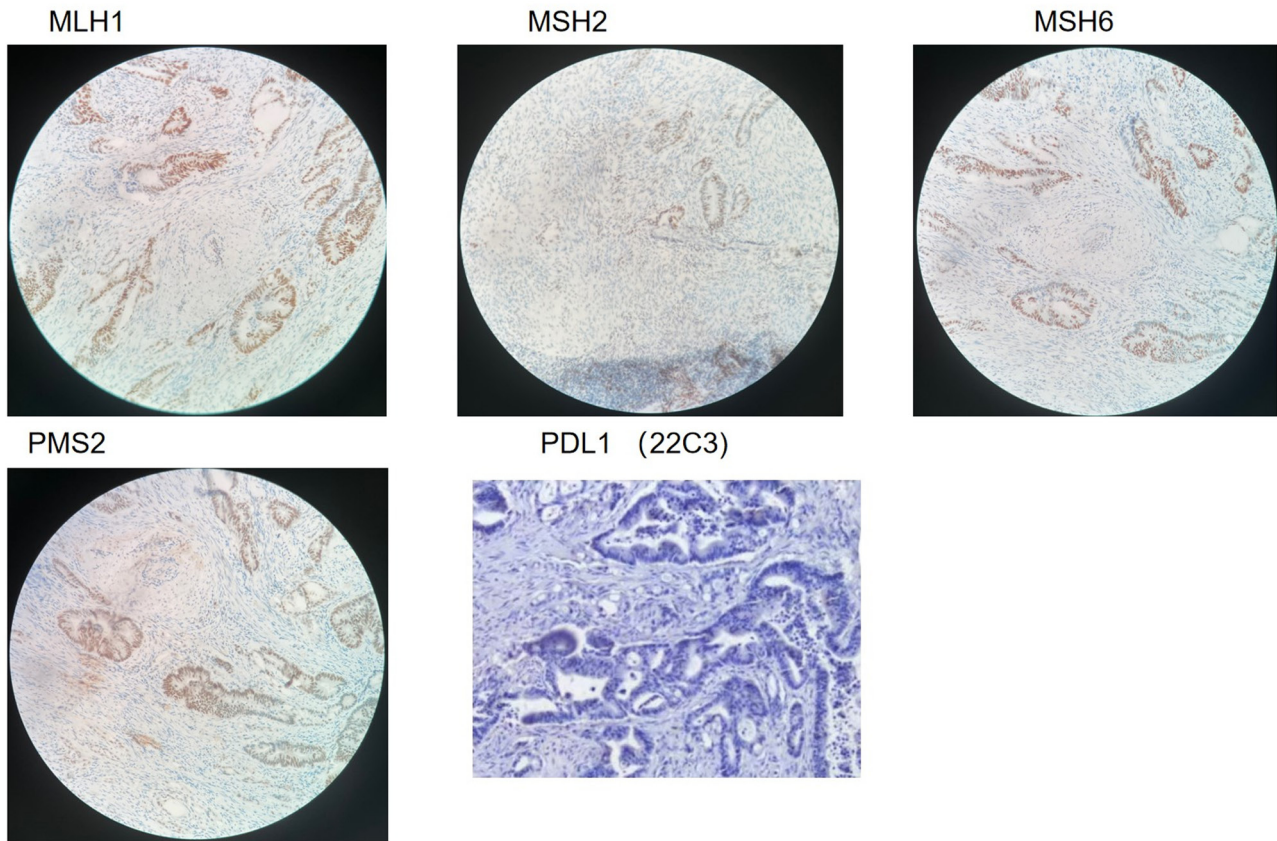


Figure 7. Immunohistochemistry results showed positive expression of the DNA mismatch repair proteins MLH1, MSH2, MSH6 and PMS2, whereas the expression of PDL1 was negative (magnification, x200). MLH1, MutL homolog 1; MSH2, MutS homolog 2; MSH6, MutS homolog 6; PMS2, PMS1 homolog 2; PDL1, programmed death-ligand 1.

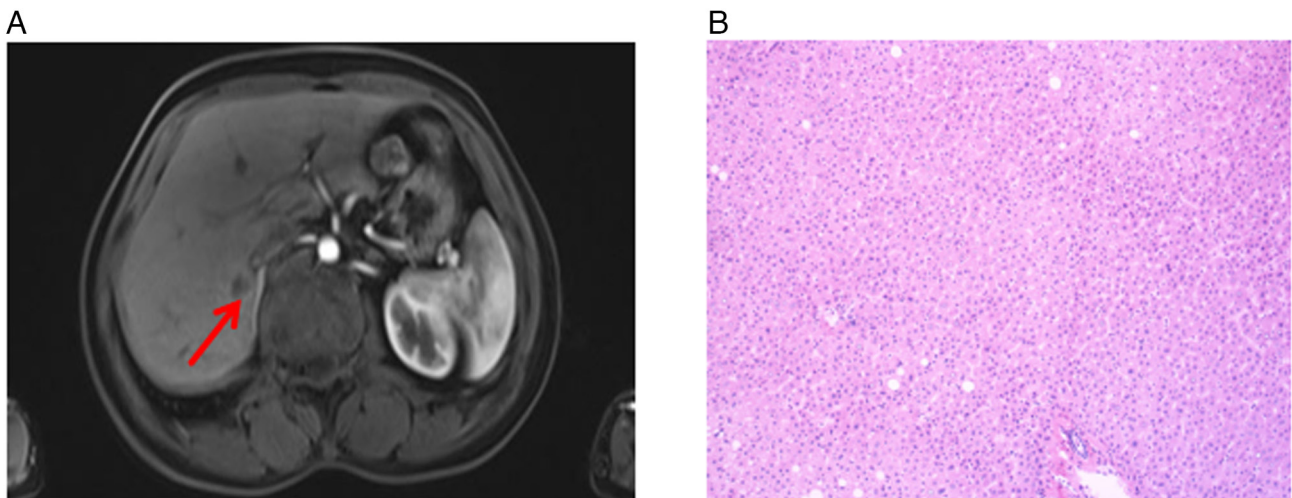


Figure 8. First liver metastasis. (A) MRI of the pelvic cavity in February 2020 showed a 1.07x0.95 cm mass in the right posterior liver (arrow) at 43 days after sigmoidectomy. (B) After six cycles of neoadjuvant chemotherapy and four cycles of bevacizumab treatment, no malignant cells were identifiable in the liver metastases resection specimen (magnification, x200).

sigmoidectomy, revealed a 1.07x0.95 cm mass in the right posterior liver (Fig. 8A). Subsequently, the patient received five cycles of neoadjuvant chemotherapy (200 mg oxaliplatin on day 1 and 2.0 g capecitabine, bid, days 1-14) and four cycles of bevacizumab (7.5 mg/kg; day 1), every three weeks as one cycle, before undergoing hepatic metastasectomy in

June 2020. During the operation, a hepatic tumor lesion was detected by B-ultrasound, but the pathologist did not find any malignant cells in the excised specimen following meticulous testing (Fig. 8B). Treatment with osimertinib (AZD9291; 80 mg/day) and bevacizumab (7.5 mg/kg; every three weeks as one cycle) was continued, whereas the colorectal

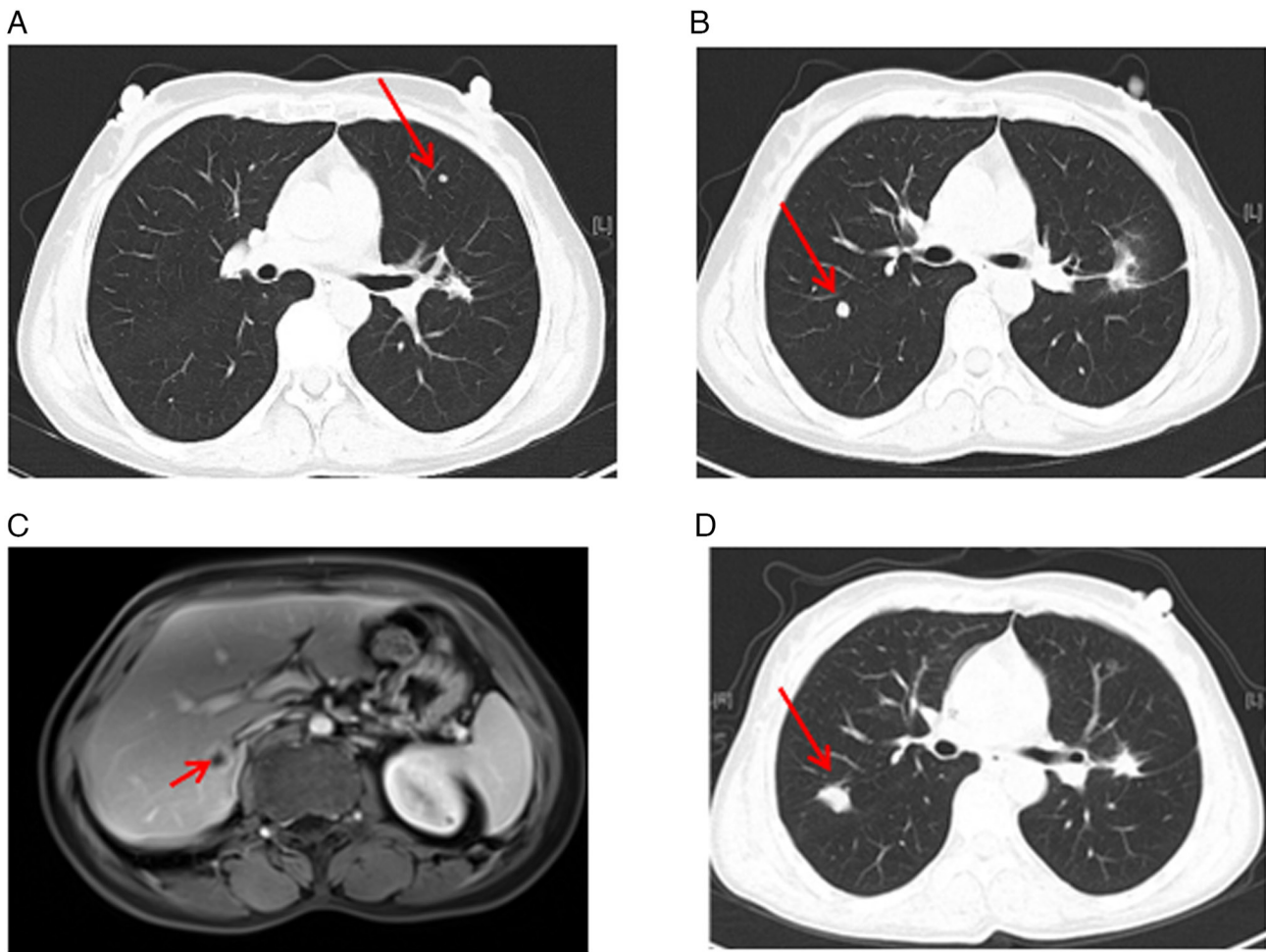


Figure 9. Enteric adenocarcinoma in right lung and the second liver metastasis. (A) Arrow points at a newly enlarged small pulmonary nodule in the right lung on thoracic contrast-enhanced CT scan in May 2021. (B) Arrow points at another newly enlarged small pulmonary nodule in the right lung on thoracic contrast-enhanced CT scan in May 2021. (C) During the routine enhanced MRI review of the abdomen in May 2021, a new lesion suggesting liver metastasis (arrow) was discovered behind the original liver metastasis. (D) A thoracic contrast-enhanced CT in February 2022 indicated good ablation on the nodule in right lung (arrow) after 10 months.

cancer-associated chemotherapy was discontinued as no colorectal cancer cells were found in the liver lesion.

A subsequent thoracic contrast-enhanced CT scan in May 2021 revealed the presence of several newly enlarged small pulmonary nodules in both lungs (Fig. 9A and B) compared with the last scan in January 2021. In addition, an abdominal and pelvic MRI identified a new abnormal focus in the right posterior lobe of the liver, indicating the presence of metastatic tumors (Fig. 9C). In May 2021, a percutaneous thoracic needle biopsy guided by MRI followed by subsequent ablation was performed to obtain tissue specimens from the largest lung nodule (Fig. 9B) which presented complete ablation in a thoracic contrast-enhanced CT in February 2022 (Fig. 9D). The biopsy revealed a small amount of adenocarcinoma tissue. IHC analysis showed weak expression of caudal type homeobox 2 (CDX2), negative expression of cytokeratin 7 (CK7), positive expression of CK20, negative Napsin A expression, partial Special AT-rich sequence-binding protein 2 (SATB2) expression and negative thyroid transcription factor 1 (TTF1) expression (Fig. 10). Based on these IHC results, the diagnosis was enteric adenocarcinoma, although the possibility of metastasis could not be ruled out. Unfortunately, the biopsy

specimen contained an insufficient quantity of tumor cells for the NGS test. The patient continued to receive treatment with oxaliplatin (200 mg on day 1), raltitrexed (5 mg on day 1) and bevacizumab (75 mg/kg; on day 1) every three weeks as one cycle for six cycles. Subsequently, the treatment regimen was adjusted to include raltitrexed, bevacizumab and osimertinib.

In February 2022, a small pulmonary nodule in the left lung showed slight enlargement in a thoracic contrast-enhanced CT scan (Fig. 11A) compared with the previous scan in May (Fig. 8A) and in November 2021, prompting an ablation procedure and a subsequent biopsy (Fig. 11B and C). The pathology report confirmed adenocarcinoma, although the primary site of origin could not be determined because of insufficient histopathologic slides for IHC and NGS. Following this, the patient continued treatment with AZD9291, bevacizumab and capecitabine up to the present time. Of note, the liver metastasis (Figs. 9C and 12A) was shown to have disappeared on the basis of an MRI examination conducted in November 2022 (Fig. 12) and at the time of conclusion of the present study (March 2023), the patient has remained alive with regular follow-up of laboratory test and CT/MRI scan.

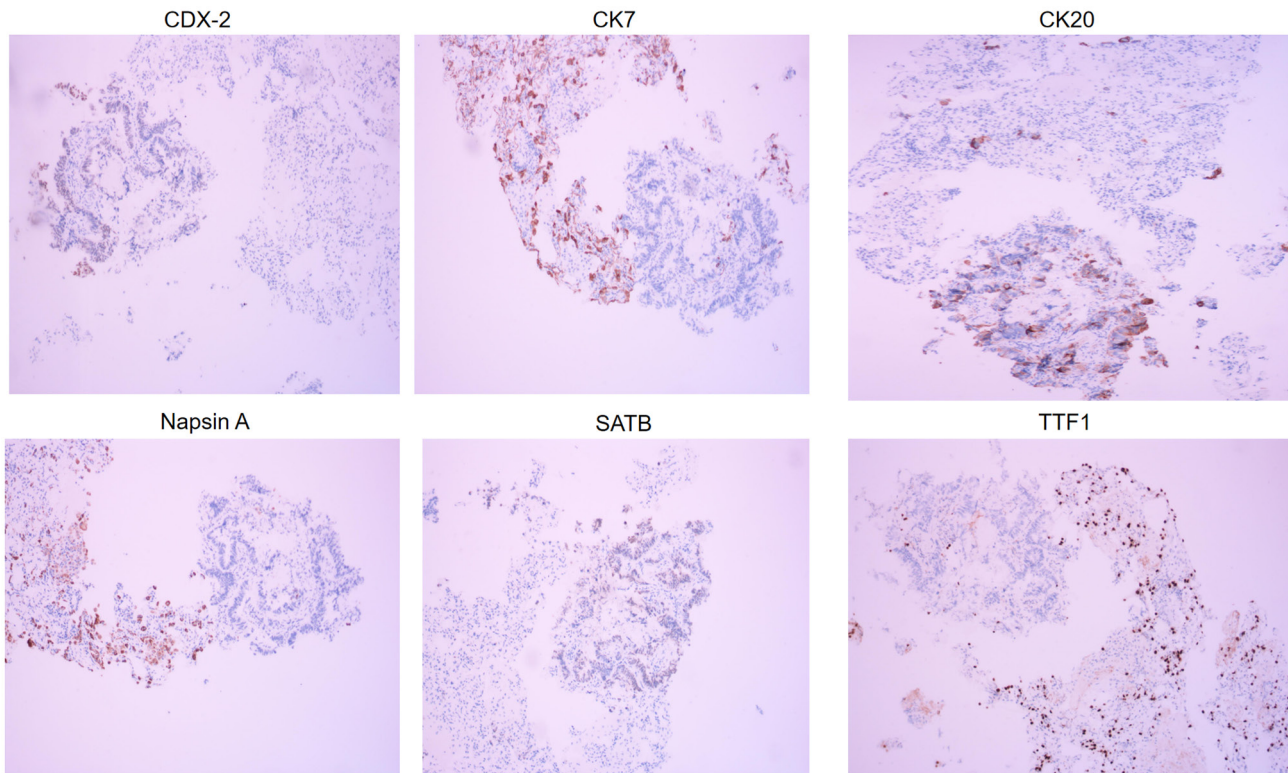


Figure 10. Immunohistochemical analysis of the specimen from the MRI-guided percutaneous thoracic needle biopsy after maintaining bevacizumab therapy for 16 months (May 2021) revealed CDX2+ (weak), CK7 (-), CK20 (+), napsin A (-), SATB2+ (partial) and TTF1 (-) staining patterns (magnification, x200), which supported metastatic enteric adenocarcinoma. CDX2, caudal type homeobox 2; CK7, cytokeratin 7; SATB2, SATB homeobox 2; TTF1, thyroid transcription factor 1.

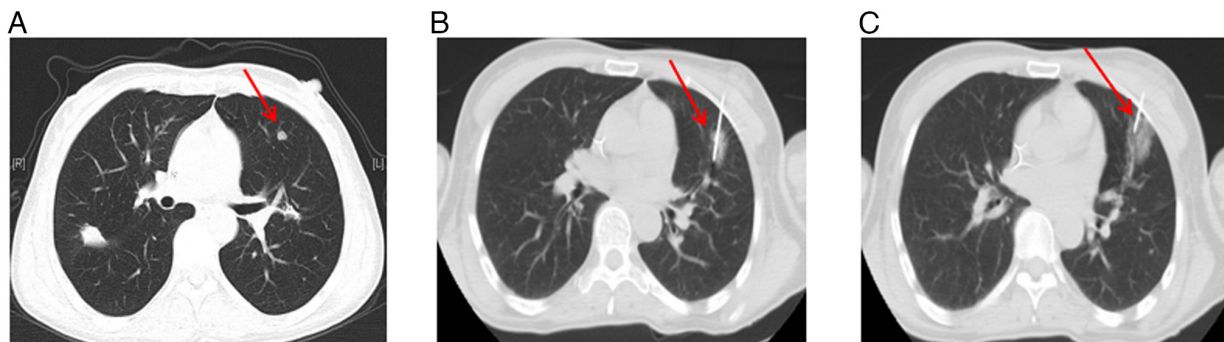


Figure 11. Enlarged nodule in the left lung and its ablation. (A) The nodule in the left lung (arrow) showed slight enlargement in February 2022. (B) Ablation site on the nodule in the left lung (arrow). (C) Biopsy site after ablation of the nodule in the left lung (arrow).

Materials and methods

Pathology. Pathological assessment was performed on the formalin-fixed, paraffin-embedded (FFPE) tissue block of operational specimens or tissue puncture needle biopsy specimens stained with hematoxylin and eosin (HE) according to standard procedures (cat. no. ab245880; Abcam) (12).

Patient and samples. Pathological samples from the patient were collected from operational specimens or puncture needle biopsy specimens. Pathological assessment was performed on tissue sections cut from FFPE tissue blocks. Tissue slides were stained with HE according to standard procedures (cat. no. ab245880; Abcam) for morphological observation.

IHC procedure. For the IHC analysis, tumor samples were obtained from the operation or using a tissue puncture needle. Tissues were immersed in 4% paraformaldehyde (Sigma-Aldrich; Merck KGaA) for 3-4 h. Dehydration was performed using a series of alcohol solutions: 75, 85 and 95% followed by anhydrous ethanol. The dehydrated tissues were embedded in paraffin and 5- μ m sections were cut as required. Paraffin sections were heated at 60°C for 20-30 min, followed by sequential treatments with xylene and an ethanol gradient. Sections were treated with a permeabilization solution (40 ml PBS + 120 μ l TritonX-100 + 400 μ l 30% H₂O₂) that had been pre-warmed to 37°C for 30 min. Antigen retrieval was performed in a solution of 0.01M sodium citrate (pH 6.0) at 90°C for 20 min. Endogenous

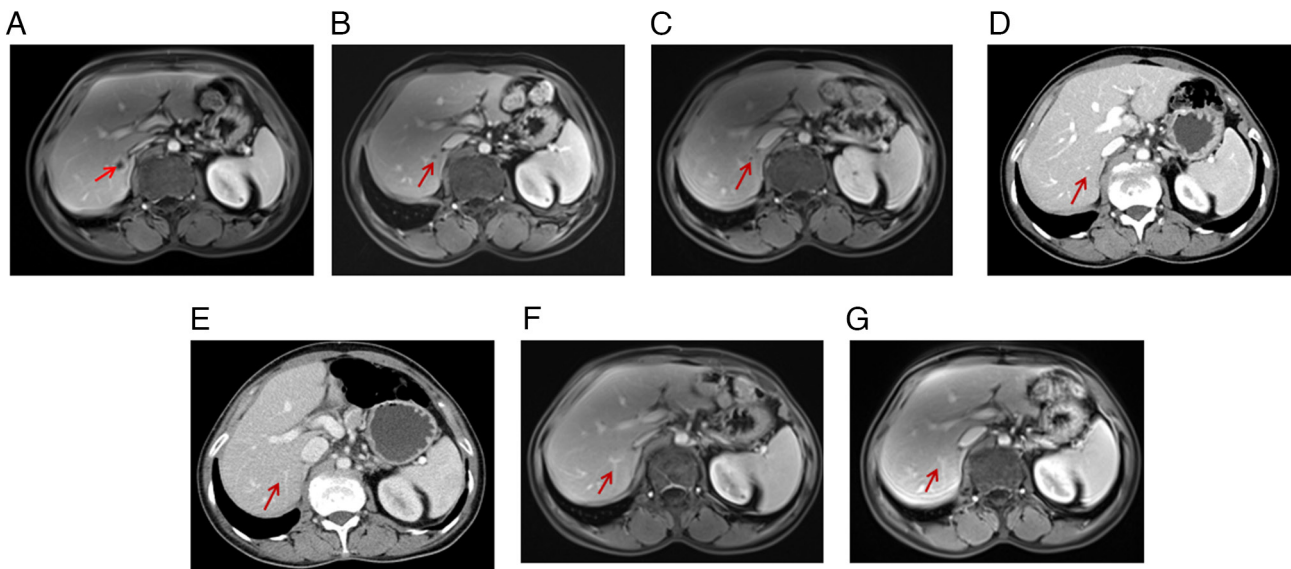


Figure 12. Abdominal MRI examination of the second lesion suggesting liver metastasis during treatment. (A) May 2021: During the routine enhanced MRI review of the abdomen, a new lesion suggesting liver metastasis (arrow) was discovered behind the original liver metastasis. (B) July 2021 and (C) September 2021: After treatment, enhanced MRI re-examinations showed that the lesion shrank gradually. (D) November 2021 and (E) February 2022: Enhanced CT re-examinations were performed, with no sign of the lesion. (F) July 2022: Enhanced MRI re-examination showed that the lesion was vaguely visible at this location. (G) November 2022: The previous lesion was not visible at all during the enhanced MRI examination. MRI, magnetic resonance imaging.

enzyme activity was deactivated with 3% H₂O₂ for 10 min at room temperature. Non-specific loci were blocked with goat serum blocking solution (cat. no. WE0320; Beijing Baiolaibo Technology Co., Ltd.) for 30 min at 37°C. Primary antibodies (e.g., anti-PD-L1 antibody; 1:1,000 dilution; cat. no. JSZ1800077; Dako North America, Inc.) were applied and incubated at 37°C for 1-2 h. After washing, HRP-conjugated secondary antibodies (HRP anti-rabbit IgG antibody; 1:500 dilution; cat. no. ab288151; Abcam) were added and incubated at 37°C for 1-2 h. Diaminobenzidine (cat. no. D12384; Sigma-Aldrich; Merck KGaA) was added for 10 min at room temperature and the reaction was observed and confirmed by microscopy.

Restaining with hematoxylin, differentiation with hydrochloric acid alcohol and dehydration were performed. Results were observed under a light microscope at x200 magnification (RX50M; Sunny Optical Technology Co., Ltd.).

For the IHC analysis with antibodies to CDX2 (cat. no. 20180310), ER (cat. no. 20173404076), CK7 (cat. no. 20180128), CK20 (cat. no. 20180074), Napsin A (cat. no. 20180102), SATB2 (cat. no. 20190103), TTF1 (cat. no. 20180077), Villin (cat. no. 20180094), MSH2 (cat. no. 20180514), MSH6 (cat. no. 20180088), PMS2 (cat. no. 20180266), MLH1 (cat. no. 20180092; all from Shanghai Gentech Co., Ltd.) and PDL1 (cat. no. JSZ1800077; Dako North America, Inc.), 5- μ m-thick sections from formalin-fixed paraffin-embedded tissues were utilized. Deparaffinization, rehydration, antigen retrieval and staining procedures followed a standard protocol (13), and negative controls were processed without the primary antibody.

DNA extraction and EGFR amplification-refractory mutation system (ARMS) mutation analysis. Genomic DNA was extracted utilizing the QIAamp DNA FFPE Tissue Kit (cat. no. 56404; Qiagen GmbH) from FFPE sections and smear

slides in accordance with the manufacturer's protocols. The elution was performed with 50 μ l Tris/Acetate/EDTA, and subsequent quantification of genomic DNA was performed using a Nano UV spectrophotometer (BSNA-101; Biolab Scientific Ltd.), ensuring optical density values at 260/280 nm fell within the range of 1.8-2.0.

For mutation analysis of the EGFR gene, an AmoyDx EGFR 29 mutations detection kit (cat. no. ADx-EG0X; Amoy Diagnostics Co., Ltd.) was employed. The DNA template, adjusted to a concentration of 2 ng/ μ l, underwent analysis on a real-time PCR instrument (PF1457N; Stratagene Mx3005P; Thermo Fisher Scientific, Inc.), following the manufacturer's instructions. Result interpretation was carried out by a technician trained to identify AmoyDx EGFR mutations. It is noteworthy that both the DNA extraction process and the ARMS method for EGFR analysis had been previously validated within our laboratory (14). Routine analysis of positive and negative controls was conducted to ensure the integrity of lab procedures.

NGS. All FFPE samples underwent independent assessment by experienced pathologists, ensuring a minimum tumor content of 20%. Subsequently, FFPE tissue sections and matched blood specimens from each patient were collected and separately processed to yield 50-250 ng of DNA per sample. Following extraction, libraries were constructed and targeted genomic regions were captured using hybridization techniques. Sequence reads were then generated using instruments from Illumina, Inc. Tumor tissue sample DNA variant testing was performed in our laboratory using published methods (14). In addition, germline mutation comparison testing was conducted on the patient's paired leukocyte DNA. Sequencing was carried out using the Cancer Sequencing YS panel, which covers the entire exonic sequences of 450 genes, the TERT promoter and introns of 39 genes. Tumor DNA was sequenced at a depth

of 1,000x, while paired leukocyte DNA was sequenced at a depth of 300x. Somatic variant types included mutations, copy number variations, as well as rearrangements and fusion events, detected using the MuTect, Pindel and EXCAVATOR tools for single nucleotide variants, insertions/deletions and copy number variations, respectively. Gene rearrangements or fusions were identified using internally developed algorithms. All variants were manually reviewed on the Integrative Genomics Viewer to ensure accuracy.

Discussion

EGFR-TKIs are the standard first-line therapy for patients with advanced or metastatic NSCLC harboring sensitive EGFR mutations (15). Osimertinib, a third-generation EGFR-TKI, has been shown to be effective as a therapy in the majority of cases of EGFR-mutated NSCLC. According to a study by Ramalingam *et al* (16), patients with exon 19Del or an L858R allele who received first-line osimertinib had a median OS of 38.6 months compared with 31.8 months in the comparative group treated with gefitinib or erlotinib, while PFS is 18.9 months compared with 10.2 months. When used as second-line treatment in patients with the T790M mutation after having received first- or second-generation EGFR-TKIs, osimertinib resulted in a PFS time of 10.1 months for T790M-positive disease (17). The median OS time is 31.8 after first-generation (16) and 36.7 months after second-generation EGFR-TKIs (18), respectively. However, almost all patients who initially responded to an EGFR-TKI eventually developed drug resistance. To extend the survival rates of patients, a promising approach is to use combination therapy of first-generation EGFR-TKIs with other therapeutic methods (19). Several prospective phase III studies have shown that this combination of chemotherapy and TKI treatment leads to a significant improvement in PFS, objective response rates and quality of life, surpassing the benefits observed with chemotherapy or EGFR-TKI alone (20).

In the present case report, the treatments were aligned with the recommendations outlined in the 2016 Guidelines of the Chinese Society of Clinical Oncology (21), which advocate for the continuation of TKI therapy for T790M-negative patients during the slowly progressive and oligoprogressive stages. The patient of the present study has undergone two chemotherapy regimens, before and after the initial administration of the first-generation TKI. Subsequently, the patient was treated with a second first-generation TKI, resulting in a 3-month PFS outcome with the emergence of a new lesion. Furthermore, a previous study reported that 21% of T790M-negative patients exhibit good efficacy when treated with AZD9291 (22). Consequently, it was chosen to administer this treatment to the patient and the results obtained were highly positive. Of note, osimertinib treatment beyond the second line of EGFR-TKI therapy showed a remarkable benefit of PFS of 63 months at the time of conclusion of the present study (March 2023) while the patient has remained alive without progression, surpassing the findings of PFS and OS in the previous studies (16,17).

Prior to 2016, in China, medical conditions prevailed where NGS genetic testing was not readily available for the majority of patients, and RT-qPCR analysis remained the primary method for checking the EGFR mutation status. In the present case, chemotherapy was administered to

reverse 1st EGFR-TKI resistance without the secondary EGFR T790M mutation ever detected by RT-qPCR (23). Subsequently, erlotinib was used, resulting in a PFS of 3 months. Of note, it has been reported that 21% of patients with T790M-negative NSCLC also exhibit sensitivity to second-line osimertinib (22). Therefore, when osimertinib became available in China, the patient of the present study was switched to osimertinib chemotherapy. The remarkable response to osimertinib prompted us to confirm the T790M-negative status. NGS was performed on the previous gefitinib- or erlotinib-resistant tumor specimens obtained from the patient, which confirmed the presence of the EGFR 19Del and T790M mutations. Of note, no other resistance genes associated with EGFR-TKI were identified by the NGS test during the course of the patient's treatment.

MWA, as a local treatment for oligoprogressive lesions, shows promise in eradicating insensitive and drug-resistant clones, potentially restoring treatment sensitivity. Furthermore, compared with surgery, MWA offers the advantage of preserving more of the normal tissue, resulting in an improved quality of life and maintaining lung function for post-procedural patients (24). The present case report provides compelling evidence that the patient benefitted from undergoing five sessions of MWA combined with chemotherapy/EGFR-TKI treatment, leading to an exceptional survival period of 110 months, far exceeding what has been reported in the literature (16,17).

The prevalence of multiple primary malignancies in cancer patients, whether in the same or different organ systems, ranges from 2-17% (25). Multiple malignancies can be categorized as synchronous or metachronous, based on their timing relative to the initial cancer diagnosis (26). In the case of the present study, the patient developed metachronous colon cancer, followed by subsequent liver and lung metastases. The occurrence of colon metastasis in lung cancer is relatively rare, with a previous study reporting only 10 cases (0.19%) out of a total of 5,239 patients with lung cancer with metastases to the colon and rectum (27). Pathology results from a colon biopsy confirmed the presence of primary colon cancer and lung metastases in this case. Radical surgery is the preferred treatment for colorectal cancer. In the present case, a synchronous liver metastasis was detected 43 days following colon cancer surgery. Following neoadjuvant chemotherapy combined with bevacizumab, the patient achieved a pathological complete response, indicating the effectiveness of the chemotherapy regimen against colon cancer. Subsequently, two oligometastases in the lung were identified during the maintenance phase of bevacizumab treatment, occurring at 16 months (May 2021) and 28 months (May 2022), respectively. The first oligometastasis was confirmed as metastatic enteric adenocarcinoma through pathological examination, whereas it could not be determined whether the second originated from the lung or intestine due to its small size. Another liver metastasis arose in May 2021. To supplement the maintenance therapy of bevacizumab and osimertinib, the patient underwent six cycles of double-drug chemotherapy. Subsequently, in line with the patient's preference, treatment continued with osimertinib, bevacizumab and capecitabine up to the present time. No sign of liver metastases was observed during the MRI examination conducted in November 2022. Throughout the disease

progression, the patient underwent repeated biopsies to assess changes in tumor pathology and to conduct genotyping for targeted therapies. As of the latest follow-up in March 2023, no recurrence has been detected in the patient.

While the reported case is promising, the diversity observed in tumor characteristics among different patients raises the need for caution in generalizing these findings to the broader population. Tumor heterogeneity encompasses variations in genetic, phenotypic and microenvironmental factors, influencing responses to treatment.

To guide clinical practice effectively, further analysis is essential to determine the degree of representativeness of the patient of the present study. This analysis should involve a larger and more diverse patient cohort, considering different tumor subtypes and clinical scenarios. In addition, exploring potential factors contributing to the observed longevity, such as specific genetic mutations or treatment responses, will provide a more comprehensive understanding. In the future, more cases will be accumulated to validate our clinical results and, where possible, conduct additional clinical research to obtain higher levels of evidence.

Of note, the present case report did have several limitations. The utilization of MWA in clinical practice for lung cancer remains limited. Thus, there is an urgent need for clinical trials to be conducted that compare the effectiveness of local ablation with other therapies, such as radiotherapy and surgery, when combined with systemic treatment for advanced cancers. The present case study, however, has offered valuable insight into the optimal approach for patients with lung cancer who have developed acquired resistance to EGFR TKIs.

In conclusion, the combination of MWA and systemic therapies has demonstrated its potential to effectively manage *in situ* oligoprogression or *ex situ* oligoprogression, and to enhance the efficacy of chemotherapy/TKI therapy in patients with NSCLC with EGFR 19Del mutations and metachronous colon adenocarcinoma. Repeated histologic biopsies and genetic testing serve as valuable indicators for adjusting treatment regimens accordingly. In addition, in cases of advanced lung cancer with a chronic course, physicians should remain vigilant regarding the occurrence and treatment of double primary carcinomas. Timely and accurate adjustments to treatment plans are expected to be of significant benefit to patients in terms of treatment efficacy and their overall quality of life.

Acknowledgements

Not applicable.

Funding

The preparation of this study was funded by the project of the investigation of factors associated with the planning system for percutaneous pulmonary microwave ablation surgery (grant no. lj007).

Availability of data and materials

The raw data of NGS can be obtained via accession no. GVM000687 under the following link: (<https://bigd.big.ac.cn/gvm/getProjectDetail?Project=GVM000687>).

Authors' contributions

YL was responsible for the conceptualization of the present study and writing the manuscript. YX, SC, JiL, FR, CX and PL acquired the majority of the data, analyzed the data, performed research of the literature and prepared the original draft. JuL was in charge of the full treatment of the patient and responsible for editing and critical review of the manuscript. YL and JuL checked and confirmed the authenticity of the raw data. All authors have read and approved the final manuscript for publication.

Ethics approval and consent to participate

The study involving a human participant was reviewed and approved by Shandong Provincial Hospital Affiliated to Shandong First Medical University, Shandong, China (approval no. 2022-061; Jinan, China). None of the treatments were experimental and written informed consent for each treatment was obtained from the patient and all procedures were conducted in accordance with the Declaration of Helsinki.

Patient consent for publication

The patient provided consent for publication of their case data and images.

Competing interests

The authors declare that they have no competing interests.

References

1. Thandra KC, Barsouk A, Saginala K, Aluru JS and Barsouk A: Epidemiology of lung cancer. *Contemp Oncol (Pozn)* 25: 45-52, 2021.
2. Schad F, Thronicke A, Steele ML, Merkle A, Matthes B, Grah C and Matthes H: Overall survival of stage IV non-small cell lung cancer patients treated with Viscum album L. in addition to chemotherapy, a real-world observational multicenter analysis. *PLoS One* 13: e0203058, 2018.
3. Billing DL and Rimner A: Results of radiation therapy as local ablative therapy for oligometastatic non-small cell lung cancer. *Cancers (Basel)* 13: 5773, 2021.
4. Wei Y, Cui Y, Guo Y, Li L and Zeng L: A lung adenocarcinoma patient with a rare EGFR E709_T710delinsD mutation showed a good response to afatinib treatment: A case report and literature review. *Front Oncol* 11: 700345, 2021.
5. Liang H, Li C, Zhao Y, Zhao S, Huang J, Cai X, Cheng B, Xiong S, Li J, Wang W, *et al*: Concomitant mutations in EGFR 19Del/L858R mutation and their association with response to EGFR-TKIs in NSCLC patients. *Cancer Manag Res* 12: 8653-8662, 2020.
6. Ettinger DS, Wood DE, Aisner DL, Akerley W, Bauman JR, Bharat A, Bruno DS, Chang JY, Chirieac LR, D'Amico TA, *et al*: Non-small cell lung cancer, version 3.2022, NCCN clinical practice guidelines in oncology. *J Natl Compr Canc Netw* 20: 497-530, 2022.
7. Pisano C, De Filippis M, Jacobs F, Novello S and Reale MLC: Management of oligoprogression in patients with metastatic NSCLC harboring ALK rearrangements. *Cancers (Basel)* 14: 718, 2022.
8. Nguyen KT, Sakthivel G, Milano MT, Qiu H and Singh DP: Oligoprogression in non-small cell lung cancer: A narrative review. *J Thorac Dis* 14: 4998-5011, 2022.
9. Shang Y, Li G, Zhang B, Wu Y, Chen Y, Li C, Zhao W and Liu J: Image-guided percutaneous ablation for lung malignancies. *Front Oncol* 12: 1020296, 2022.
10. Wei Z, Ye X, Yang X, Zheng A, Huang G, Li W, Wang J, Han X, Meng M and Ni Y: Microwave ablation combined with EGFR-TKIs versus only EGFR-TKIs in advanced NSCLC patients with EGFR-sensitive mutations. *Oncotarget* 8: 56714-56725, 2017.

11. Mirsadraee S, Oswal D, Alizadeh Y, Caulo A and van Beek E Jr: The 7th lung cancer TNM classification and staging system: Review of the changes and implications. *World J Radiol* 4: 128-134, 2012.
12. Feldman AT and Wolfe D: Tissue processing and hematoxylin and eosin staining. *Methods Mol Biol* 1180: 31-43, 2014.
13. Magaki S, Hojat SA, Wei B, So A and Yong WH: An introduction to the performance of immunohistochemistry. *Methods Mol Biol* 1897: 289-298, 2019.
14. Liu J, Zhao R, Zhang J and Zhang J: ARMS for EGFR mutation analysis of cytologic and corresponding lung adenocarcinoma histologic specimens. *J Cancer Res Clin Oncol* 141: 221-227, 2015.
15. Nan X, Xie C, Yu X and Liu J: EGFR TKI as first-line treatment for patients with advanced EGFR mutation-positive non-small-cell lung cancer. *Oncotarget* 8: 75712-75726, 2017.
16. Ramalingam SS, Vansteenkiste J, Planchard D, Cho BC, Gray JE, Ohe Y, Zhou C, Reungwetwattana T, Cheng Y, Chewaskulyong B, *et al*: Overall survival with osimertinib in untreated, EGFR-mutated advanced NSCLC. *N Engl J Med* 382: 41-50, 2020.
17. Mok TS, Wu YL, Ahn MJ, Garassino MC, Kim HR, Ramalingam SS, Shepherd FA, He Y, Akamatsu H, Theelen WS, *et al*: Osimertinib or platinum-pemetrexed in EGFR T790M-positive lung cancer. *N Engl J Med* 376: 629-640, 2017.
18. Mok TS, Cheng Y, Zhou X, Lee KH, Nakagawa K, Niho S, Lee M, Linke R, Rosell R, Corral J, *et al*: Improvement in overall survival in a randomized study that compared dacomitinib with gefitinib in patients with advanced non-small-cell lung cancer and EGFR-activating mutations. *J Clin Oncol* 36: 2244-2250, 2018.
19. Zhou Q, Xu CR, Cheng Y, Liu YP, Chen GY, Cui JW, Yang N, Song Y, Li XL, Lu S, *et al*: Bevacizumab plus erlotinib in Chinese patients with untreated, EGFR-mutated, advanced NSCLC (ARTEMIS-CTONG1509): A multicenter phase 3 study. *Cancer Cell* 39: 1279-1291.e3, 2021.
20. Wu Q, Luo W, Li W, Wang T, Huang L and Xu F: First-generation EGFR-TKI plus chemotherapy versus EGFR-TKI alone as first-line treatment in advanced NSCLC with EGFR activating mutation: A systematic review and meta-analysis of randomized controlled trials. *Front Oncol* 11: 598265, 2021.
21. Chinese Society of Clinical Oncology: Guidelines of Chinese Society of Clinical Oncology (CSCO) Primary Lung Cancer 2016.V1. People's Medical Publishing House, Beijing, China. <https://meeting.cSCO.org.cn/pdf/web/viewer.html?file=/upload/Periodical/201811/201811965213.pdf> Accessed November 9, 2018 (In Chinese).
22. Jänne PA, Yang JC, Kim DW, Planchard D, Ohe Y, Ramalingam SS, Ahn MJ, Kim SW, Su WC, Horn L, *et al*: AZD9291 in EGFR inhibitor-resistant non-small-cell lung cancer. *N Engl J Med* 372: 1689-1699, 2015.
23. Xia GH, Zeng Y, Fang Y, Yu SR, Wang L, Shi MQ, Sun WL, Huang XE, Chen J and Feng JF: Effect of EGFR-TKI retreatment following chemotherapy for advanced non-small cell lung cancer patients who underwent EGFR-TKI. *Cancer Biol Med* 11: 270-276, 2014.
24. Lin M, Eiken P and Blackmon S: Image guided thermal ablation in lung cancer treatment. *J Thorac Dis* 12: 7039-7047, 2020.
25. Vogt A, Schmid S, Heinimann K, Frick H, Herrmann C, Cerny T and Omlin A: Multiple primary tumours: Challenges and approaches, a review. *ESMO Open* 2: e000172, 2017.
26. Pan SY, Huang CP and Chen WC: Synchronous/metachronous multiple primary malignancies: Review of associated risk factors. *Diagnostics (Basel)* 12: 1940, 2022.
27. Gonzalez-Tallon AI, Vasquez-Guerrero J and Garcia-Mayor MA: Colonic metastases from lung carcinoma: A case report and review of the literature. *Gastroenterology Res* 6: 29-33, 2013.



Copyright © 2024 Li *et al*. This work is licensed under a Creative Commons Attribution-NonCommercial-NoDerivatives 4.0 International (CC BY-NC-ND 4.0) License.